

Articles

Magnetochemistry of Tetrahaloferrate(III) Ions. 5. Specific Heats of and Magnetic Ordering in [4-Cl(py)H]₃Fe₂Br₉, [4-Br(py)H]₃Fe₂Br₉, and [4-Cl(py)H]_{1.1}[4-Br(py)H]_{1.9}Fe₂Br₉

Roey Shaviv, Carol B. Lowe, and Richard L. Carlin*

Department of Chemistry, University of Illinois at Chicago, Chicago, Illinois 60680

Received June 11, 1992

Specific heats of the three title materials and the magnetic susceptibilities of the last two substances are reported. These materials are part of a series of canted antiferromagnets that have the same general formula and which may be assumed to be isomorphous. All three substances display two closely-spaced λ -anomalies in their specific heats, with ordering temperatures of 5.50 and 7.92 K for [4-Cl(py)H]₃Fe₂Br₉, 5.23 and 7.635 K for [4-Br(py)H]₃Fe₂Br₉, and 7.52 and 7.80 K for [4-Cl(py)H]_{1.1}[4-Br(py)H]_{1.9}Fe₂Br₉. Magnetic susceptibility measurements reveal ordering temperatures at 7.73 and 7.78 K for [4-Cl(py)H]_{1.1}[4-Br(py)H]_{1.9}Fe₂Br₉, whereas [4-Cl(py)H]₃Fe₂Br₉ and [4-Br(py)H]₃Fe₂Br₉ display but a single ordering temperature each, at 7.96 and 7.70 K, respectively. The ordering phenomena are three-dimensional in nature, and the magnetic entropies are in excellent agreement with the theoretical predictions. Effects of chemical substitutions on possible exchange pathways are discussed.

Introduction

There is a large series of compounds of the stoichiometry A₃-Fe₂X₉, where A may be a pyridinium or 4-X-pyridinium cation and X may be chloride, bromide, or a homogeneous mixture of the two. A number of studies on these materials have shown that they all contain the tetrahedral tetrahaloferrate(III) ion and that they may best be formulated, for example, in the case of [4-Cl(py)H]₃Fe₂Br₉, as 2[4-Cl(py)H][FeBr₄].[4-Cl(py)H]Br.¹⁻⁶ By contrast, most of the transition metal and lanthanide compounds of the stoichiometry A₃M₂X₉ contain the dimeric [M₂X₉]³⁻ ion. The intradimer magnetic exchange in the latter materials has been studied extensively, but the interdimer interactions are weak. Most of the tetrahaloferrate(III) materials, in addition to their unexpected structure, undergo long-range order in an easily-accessible temperature region as canted antiferromagnets. This latter point was not anticipated, for the high-spin iron(III) ion has a ⁶A₁ ground state, which lacks appreciable anisotropy.^{4,7}

As mentioned above, many stoichiometric substitutions can be made with this series of compounds, which opens up a variety of studies to try to elucidate their behavior. The crystal structures of several compositions are known. Thus, [4-Cl(py)H]₃Fe₂Br₉, [4-Cl(py)H]₃Fe₂Cl₉, [4-Br(py)H]₃Fe₂Cl₉, and [4-Br(py)H]₃Fe₂-Cl_{1.3}Br_{7.7} are all monoclinic and isomorphous,^{1,2} [(py)H]₃Fe₂Cl₉ is orthorhombic,³ and [(py)H]₃Fe₂Br₉ is monoclinic but is not isomorphous with the others.⁸ We expect [4-Br(py)H]₃Fe₂Br₉ and [4-Cl(py)H]_{1.1}[4-Br(py)H]_{1.9}Fe₂Br₉ to be monoclinic as well and isomorphous with the first four compositions.

The magnetic interactions in these materials depend greatly on the chemical composition and in particular on the halide anion. Materials whose halide anion is the smaller chloride tend to order as canted antiferromagnets below 3 K, while the bromide

analogues display a more complex ordering behavior at higher temperatures. All known compositions in this chemical system (with the exception of [(py)H]₃Fe₂Br₉⁸) order as canted antiferromagnets. In this paper we characterize the unusual magnetic ordering in the three title compositions, all tetrabromoferrates(III).

Experimental Section

The mixed-cation material [4-Cl(py)H]_{1.1}[4-Br(py)H]_{1.9}Fe₂Br₉ was prepared by adding equimolar portions of 4-chloropyridinium chloride and 4-bromopyridinium chloride, each to chloroform in two different separatory funnels. With the addition of a saturated solution of NaHCO₃, 4-halopyridine formed with effervescence and dissolved in the organic layer. To the separated organic layer was added 4 M HBr in excess. The [4-X(py)H]Br which formed was soluble in the aqueous layer. The separate halopyridinium bromide solutions were mixed, and a solution of FeBr₃ in 4 M HBr was added. Slow evaporation over approximately 2 weeks led to large, red-black single crystals. Anal. Calc (found): C, 14.31, 14.26; H, 1.20, 1.19; Br, 69.18, 69.40; Cl, 3.10, 3.06; Fe, 8.87, 8.80; N, 3.34, 3.35. [4-Br(py)H]₃Fe₂Br₉ was prepared in a similar manner and resulted in large red-black single crystals, which were collected by filtration and dried in vacuo. Anal. Calc for C₁₅H₁₅N₃Fe₂Br₁₂: C, 13.78; H, 1.16; Br, 73.32; Fe, 8.54; N, 3.21. Found: C, 13.54; H, 1.08; Br, 74.29; Fe, 8.40; N, 3.14. Large single crystals of [4-Cl(py)H]₃Fe₂Br₉ were prepared and characterized as previously described.²

Specific heat measurements, between 1.6 and 12 K for [4-Cl(py)H]_{1.1}[4-Br(py)H]_{1.9}Fe₂Br₉, between 1.5 and 39 K for [4-Cl(py)H]₃Fe₂Br₉, and between 1.8 and 38 K for [4-Br(py)H]₃Fe₂Br₉ were made in the quasi-adiabatic calorimetric cryostat that was described in a separate communication.⁵ *ac* magnetic susceptibility measurements for [4-Cl(py)H]_{1.1}[4-Br(py)H]_{1.9}Fe₂Br₉ between 1.13 and 4.2 K were conducted in two orientations on a single-crystal specimen. Measurements between 4.0 and 22.0 K were conducted in another apparatus at only one orientation. Three crystal orientations were studied in the *ac* susceptibility experiments on a 0.0953-g single-crystal specimen of [4-Br(py)H]₃Fe₂Br₉ using the same apparatus.

Results

(a) [4-Cl(py)H]_{1.1}[4-Br(py)H]_{1.9}Fe₂Br₉. We assume that the substance is isomorphous with both [4-Cl(py)H]₃Fe₂Br₉ and the related salts reported earlier.^{1,2} The morphology and chemical nature of the material are consistent with this unremarkable hypothesis. The magnetic susceptibility data of a single-crystal

- (1) Zora, J. A.; Seddon, K. R.; Hitchcock, P. B.; Lowe, C. B.; Shum, D. P.; Carlin, R. L. *Inorg. Chem.* **1990**, *29*, 3302.
- (2) Lowe, C. B.; Carlin, R. L.; Schultz, A. J.; Loong, C.-K. *Inorg. Chem.* **1990**, *29*, 3308.
- (3) Lowe, C. B. Dissertation, University of Illinois at Chicago, 1990.
- (4) Carlin, R. L.; Lowe, C. B.; Palacio, F. *An. Quim.* **1991**, *87*, 5.
- (5) Shaviv, R.; Merabet, K. E.; Shum, D. P.; Lowe, C. B.; Gonzalez, D.; Burriel, R.; Carlin, R. L. *Inorg. Chem.* **1992**, *31*, 1724.
- (6) Shaviv, R.; Carlin, R. L. *Inorg. Chem.* **1992**, *31*, 710.
- (7) Carlin, R. L. *Magnetochemistry*; Springer-Verlag: Berlin, 1986.
- (8) Lowe, C. B.; Schultz, A. J.; Shaviv, R.; Carlin, R. L. To be published.

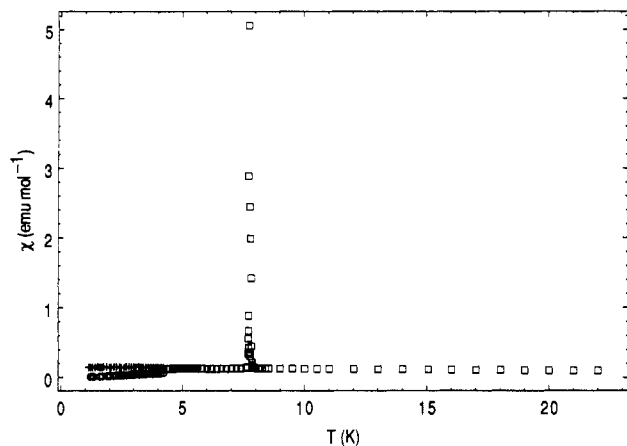


Figure 1. Susceptibility measurements for $[4\text{-Cl(py)H}]_{1.1}[4\text{-Br(py)H}]_{1.9}\text{Fe}_2\text{Br}_9$.

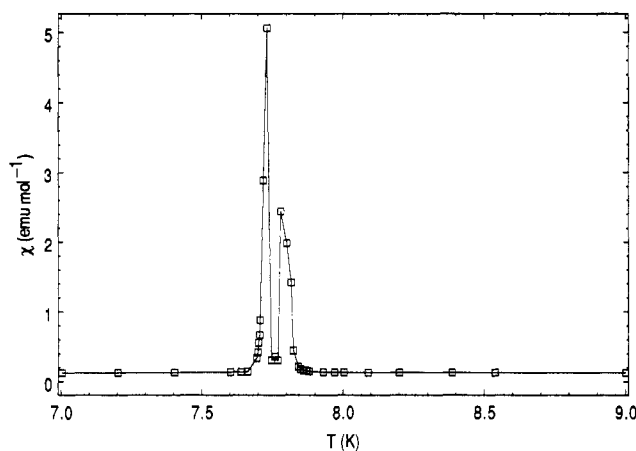


Figure 2. Expanded version of susceptibility data for $[4\text{-Cl(py)H}]_{1.1}[4\text{-Br(py)H}]_{1.9}\text{Fe}_2\text{Br}_9$.

sample, given in Figure 1, indicate that this compound is likewise a canted antiferromagnet. Under higher resolution (Figure 2), the ferromagnetic spike may be resolved into two peaks with maxima occurring at 7.73 and 7.78 K. Strong absorption⁷ (or out-of-phase signal, χ'') was observed in the transition region.

These results are confirmed by the specific heat data presented in Figure 3, which exhibit two sharp peaks at 7.52 and 7.80 K. The temperature of the first transition is lower in the specific heat experiment than in the magnetic susceptibility one, a change which is attributed to the different treatments of the samples in the two experiments. A single-crystal sample was used for the susceptibility measurements whereas a powdered sample was pressed into a pellet prior to the specific heat measurements. The same kind of decrease in transition temperature was observed for other compounds in this chemical system.^{5,6} The discrepancy is assumed to have no physical significance.

(b) $[4\text{-Cl(py)H}]_3\text{Fe}_2\text{Br}_9$. The specific heat of $[4\text{-Cl(py)H}]_3\text{Fe}_2\text{Br}_9$ between 1.5 and 39 K, presented in Figure 4, is observed to exhibit two λ -type peaks, at 5.50 and 7.92 K. The transition at 7.92 K is in good agreement with the weak ferromagnetic peak observed in the *ac* susceptibility data.² The susceptibility data provide no indication concerning the existence of the 5.50 K transition. The specific heat above the transitions behaves similarly to that of analogous compositions.

(c) $[4\text{-Br(py)H}]_3\text{Fe}_2\text{Br}_9$. The *ac* susceptibility data at zero applied field of a single crystal of $[4\text{-Br(py)H}]_3\text{Fe}_2\text{Br}_9$ are presented in Figure 5. Data were taken at three crystal orientations. The telling ferromagnetic peak is observed at 7.73 K with the field parallel to the *b* crystallographic axis, as for similar compounds in this system. A strong out-of-phase signal is also observed at this temperature. The easy axis for antifer-

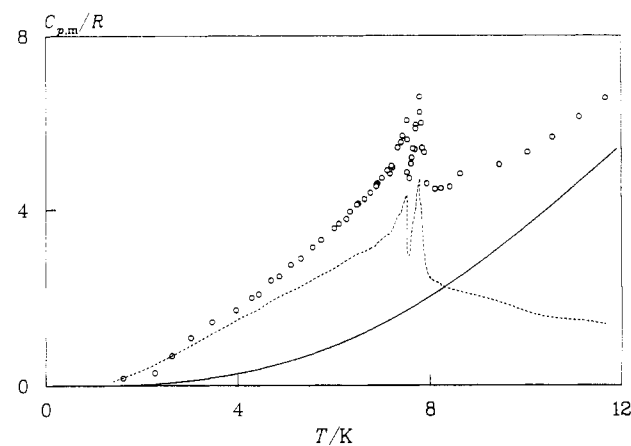


Figure 3. Specific heat of $[4\text{-Cl(py)H}]_{1.1}[4\text{-Br(py)H}]_{1.9}\text{Fe}_2\text{Br}_9$. The solid curve is the calculated lattice heat capacity, and the dashed curve is the magnetic contribution. (The choppiness of the latter curve is an artifact).

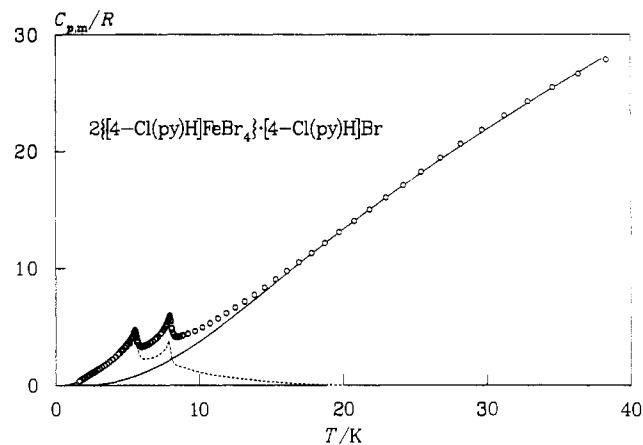


Figure 4. Specific heat of $[4\text{-Cl(py)H}]_3\text{Fe}_2\text{Br}_9$. The solid curve is the calculated lattice contribution, and the dashed curve is the derived magnetic specific heat.

romagnetic ordering appears to be the *c* crystallographic axis. A ferromagnetic peak is also present in data taken with the magnetic field parallel to the *a* crystallographic axis, due to misalignment in the *ab* plane. This magnetic behavior is almost identical to that displayed by $[4\text{-Cl(py)H}]_3\text{Fe}_2\text{Br}_9$.²

The specific heat of $[4\text{-Br(py)H}]_3\text{Fe}_2\text{Br}_9$ is presented in Figure 6. Two λ -type transitions associated with magnetic ordering are identifiable at 5.23 and 7.635 K.

Discussion

Lattice Contribution. A determination of the lattice contribution to the specific heat is required in order to resolve the experimental data and to analyze the magnetic ordering. The lattice specific heats were determined using the enhanced version⁵ of the Komada–Westrum phonon distribution model⁹ in a manner similar to that used in the analysis of the specific heat of other compounds in the series.^{5,6} The model utilizes specific heat data along with structural and chemical parameters to calculate an approximate phonon distribution function, which is represented by the apparent characteristic temperature, Θ_{KW} . This approach provides a significant improvement over the commonly used Debye model. Thus, Θ_{KW} values for $[4\text{-Cl(py)H}]_3\text{Fe}_2\text{Br}_9$ and $[4\text{-Br(py)H}]_3\text{Fe}_2\text{Br}_9$ were calculated, on the basis of experimental data. The lattice contributions to the specific heats of these substances were then determined using the respective parameters 31.9 and

(9) Komada, N. Dissertation, University of Michigan, 1985; Komada, N.; Westrum, E. F., Jr. *Thermochim. Acta* 1988, 109, 11; Komada, N.; Moecher, D. P.; Westrum, E. F., Jr.; Hemingway, B. S.; Zolotov, Y. M.; Semenov, Y. V.; Khodakovskiy, I. L. *J. Chem. Thermodyn.*, submitted for publication.

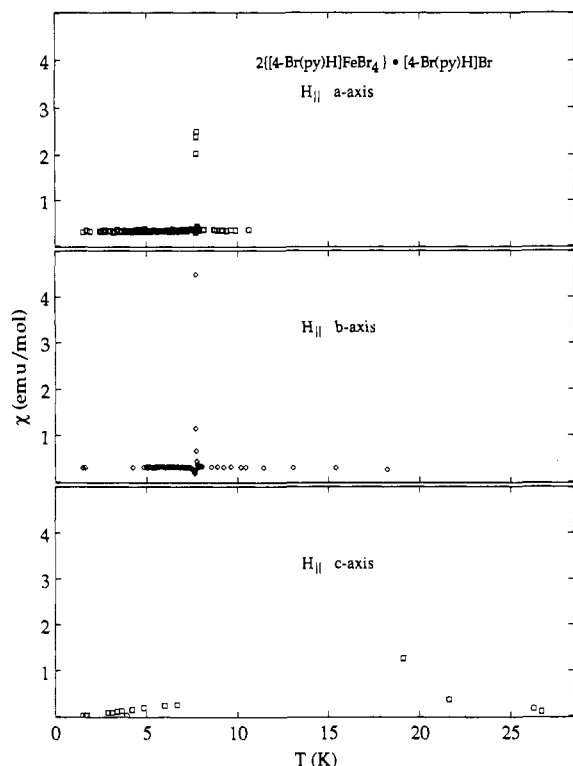


Figure 5. *ac* Susceptibility data for $[4\text{-Br(py)H}]_3\text{Fe}_2\text{Br}_9$. Portions of three data sets are shown.

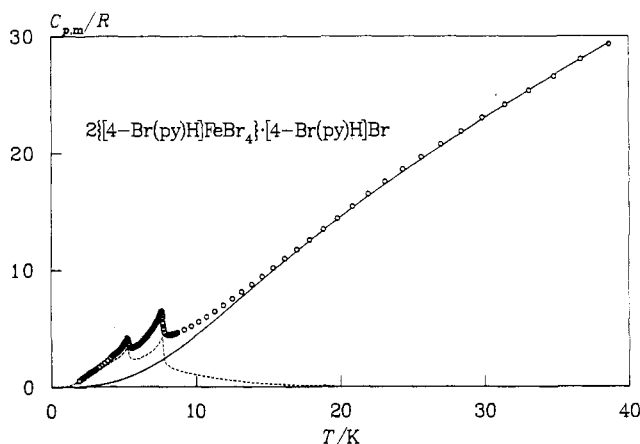


Figure 6. Specific heat of $[4\text{-Br(py)H}]_3\text{Fe}_2\text{Br}_9$. The solid curve is the calculated lattice contribution, and the dashed curve is the derived magnetic specific heat.

22.87 K, which are the constant values of the apparent characteristic temperatures above 19 K. (A constant Θ_{KW} , as a function of temperature, implies that the experimental specific heat consists only of the lattice contribution.)

An independent determination of Θ_{KW} for $[4\text{-Cl(py)H}]_{1.1}[4\text{-Br(py)H}]_{1.9}\text{Fe}_2\text{Br}_9$ was precluded because experimental data above 12 K are not available. Thus the characteristic temperature was determined using the relation $\Theta_{\text{KW}}([4\text{-Cl(py)H}]_{1.1}[4\text{-Br(py)H}]_{1.9}\text{Fe}_2\text{Br}_9) = \{1.1 \Theta_{\text{KW}}([4\text{-Cl(py)H}]_3\text{Fe}_2\text{Br}_9) + 1.9 \Theta_{\text{KW}}([4\text{-Br(py)H}]_3\text{Fe}_2\text{Br}_9)\}/3 = 26.2$ K. A similar method has been used in the evaluation of specific heat contributions to the lanthanide sesquisulfides.¹⁰ The lattice specific heats are plotted in Figures 3, 4, and 6.

Magnetic Phenomena: Analysis of the Transitions. (a) $[4\text{-Cl(py)H}]_{1.1}[4\text{-Br(py)H}]_{1.9}\text{Fe}_2\text{Br}_9$. As for the other $[4\text{-X(py)H}]_3\text{Fe}_2\text{X}_9$ compositions, the manifestation of magnetic ordering is

associated with a sharp peak in the magnetic susceptibility which is accompanied with a strong out-of-phase signal, χ'' . Such behavior is typical of spin canting and was interpreted as such in related compositions.¹⁻⁶ However, unlike those of most other materials in this chemical system, the ferromagnetic peak in the magnetic susceptibility of $[4\text{-Cl(py)H}]_{1.1}[4\text{-Br(py)H}]_{1.9}\text{Fe}_2\text{Br}_9$ (Figures 1 and 2) can clearly be resolved into two separate peaks, indicating two ordering temperatures and thus two canted phases. The same phenomena are mirrored in the specific heat data (Figure 3).

For the purpose of determining the thermodynamic functions of $[4\text{-Cl(py)H}]_{1.1}[4\text{-Br(py)H}]_{1.9}\text{Fe}_2\text{Br}_9$, the experimental specific heat was extrapolated to 0 K by using the data up to 4.4 K to derive an energy distribution function, which was then used to reproduce the experimental results up to that temperature, as well as to perform the extrapolation. The extrapolation was made under the constraint of a T^3 dependence approaching 0 K. Thermodynamic functions were then determined by fitting the extrapolated specific heat and the experimental data between 0 and 7 K and between 8.2 and 12 K to two polynomial functions and integrating. A manual integration was used over the transition region, between 7 and 8.2 K. The total entropy at 12 K was determined as $5.31R$ whereas the lattice entropy at that temperature was found to be $2.38R$. The magnetic entropy at 12 K is therefore $2.93R$. At 7.52 K, the first critical temperature, the total and lattice entropies are $2.80R$ and $0.65R$, respectively. Thus the magnetic entropy at that temperature is $2.15R$, representing 61% of the theoretical magnetic entropy, $2R \ln(2 \times 5/2 + 1) = 3.58R$. At 7.80 K, the second critical temperature, the total and the lattice entropies are $3.12R$ and $0.73R$, respectively. Thus the magnetic entropy at that temperature is $2.39R$, which is 71% of the total magnetic entropy of the system. At 12 K, 82% of the theoretical entropy is accounted for.

The entropy distribution and in particular the relatively large degree of magnetic ordering at the second critical temperature (71%) strongly support the notion that cooperative three-dimensional exchange effects are the prime interactions in this material. By contrast, evidence of substantial short-range order is seen for the compounds $(\text{pyH})_3\text{Fe}_2\text{Br}_9$,⁸ $[4\text{-Br(py)H}]_3\text{Fe}_2\text{Cl}_9$,⁶ and $(\text{pyH})_3\text{Fe}_2\text{Cl}_9$ ¹¹ but not for $[4\text{-Cl(py)H}]_3\text{Fe}_2\text{Cl}_9$.⁵ None of these other materials display two transitions as do the two substances reported here. Two critical temperatures, and somewhat more complicated exchange interactions, are also observed in the magnetic susceptibilities of single crystals of $[4\text{-Br(py)H}]_3\text{Fe}_2\text{Cl}_9\text{Br}_{7.7}$.² Large, homogeneous, single-phase single crystals readily form in all these stoichiometries.

(b) $[4\text{-Cl(py)H}]_3\text{Fe}_2\text{Br}_9$. The analysis of the magnetic specific heat was accomplished in a manner similar to that used in the previous section. Thus the experimental specific heat was extrapolated to 0 K by using the data between 1.5 and 2.2 K to calculate a distribution function which in turn was used to reproduce the data up to that temperature and for the extrapolation. Thermodynamic functions were determined by fitting the extrapolated specific heat and the experimental data to six polynomial segments and integrating. At the first transition temperature, $T_{c1} = 5.50$ K, the total, lattice and magnetic entropies are $2.159R$, $0.224R$, and $1.935R$, respectively. At the second transition temperature, $T_{c2} = 7.92$ K, these values are $3.627R$, $0.719R$, and $2.908R$, respectively. The tail of the transition extends to about 19 K, where the entropy values are $9.809R$, $6.234R$, and $3.575R$. Above 19 K, the agreement between the lattice contribution and the experimental specific heat is within experimental error (Figure 4). The acquired magnetic entropy represents 54% and 81% of the theoretical entropy for the system at 5.50 and 7.92 K, respectively. The magnetic entropy at 19 K is in excellent agreement with the theoretical value.

(10) Shaviv, R. Thesis, University of Michigan, 1988. Shaviv, R.; Westrum, E. F., Jr.; Gruber, J. B.; Palmer, P. E. *J. Chem. Phys.*, in press.

(11) Shaviv, R.; Lowe, C. B.; Zora, J. A.; Aakerøy, C. B.; Hitchcock, P. B.; Seddon, K. R.; Carlin, R. L. *Inorg. Chim. Acta* 1992, 198-200, 1992.

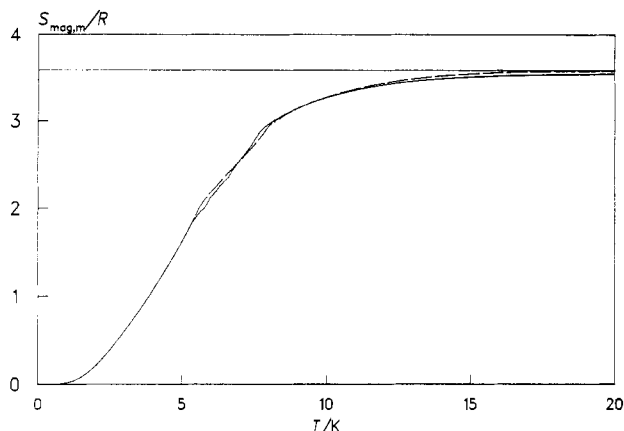


Figure 7. Magnetic entropies of [4-Br(py)H]₃Fe₂Br₉ (solid curve) and [4-Cl(py)H]₃Fe₂Br₉ (dashed curve). The horizontal line represents the theoretical magnetic entropy for the system.

As in [4-Cl(py)H]_{1.1}[4-Br(py)H]_{1.9}Fe₂Br₉, most of the magnetic ordering is completed at the second critical temperature (81%), which implies that the magnetic interactions are governed by long-range three-dimensional exchange. Short-range exchange interaction plays a smaller role in this material than in any other composition yet examined in this chemical system. These observations are consistent with the magnetic susceptibility data, which are found to be reproducible by the simple cubic Heisenberg AF model with $J/k_B = -0.47$ K and $g = 1.98$.²

Finding two λ -type transitions, at 5.50 and 7.92 K, in the specific heat of this composition was not expected, for ac susceptibility data give no indication of the transition at 5.50 K.² These single-crystal ac susceptibility data along both the a and b crystallographic axes are constant between 4.8 and 6.5 K, while data along the c axis (the easy axis) are available only below 4.2 K. Thus [4-Cl(py)H]₃Fe₂Br₉, like [4-Cl(py)H]_{1.1}[4-Br(py)H]_{1.9}Fe₂Br₉, undergoes two ordering transitions, and two distinct ordered phases are present. The higher critical temperatures, T_{c2} , are almost identical for the two materials (7.92 K for [4-Cl(py)H]₃Fe₂Br₉ and 7.80 K for [4-Cl(py)H]_{1.1}[4-Br(py)H]_{1.9}Fe₂Br₉). For both compositions, this transition is associated with the same phenomenon, i.e., long-range antiferromagnetic order (c being the easy axis) accompanied by canting of the magnetic moments toward the b axis.

The transition at lower temperatures, T_{c1} , appears to be associated with different phenomena in [4-Cl(py)H]₃Fe₂Br₉ and in [4-Cl(py)H]_{1.1}[4-Br(py)H]_{1.9}Fe₂Br₉. On the basis of the value $T_{c1} = 5.50$ K, we calculate a magnetic exchange constant, $J/k_B = -0.22$ K.

(c) [4-Br(py)H]₃Fe₂Br₉. The thermodynamic functions of [4-Br(py)H]₃Fe₂Br₉ were determined by the same method used for the other two compositions. At the first critical temperature, $T_{c1} = 5.23$ K, the lattice and total specific heats are $0.819R$ and $4.210R$, respectively. The corresponding entropies are $0.245R$ and $2.009R$, respectively. Thus the magnetic specific heat and entropy at T_{c1} are $3.391R$ and $1.764R$ (56% of the theoretical value), respectively. At the second critical temperature, T_{c2} , the lattice and the total specific heats are $2.316R$ and $6.576R$, respectively. The corresponding entropies are $0.795R$ and $3.641R$. The magnetic specific heat and the magnetic entropy at T_{c2} are, therefore, $4.260R$ and $2.846R$ (79% of $3.584R$).

The magnetic entropy at 19 K is $3.534R$, representing 99% of the theoretical magnetic entropy for the system. The agreement between the experimental values and the calculated lattice contribution is within experimental uncertainty above about 19 K. The magnetic entropies of [4-Cl(py)H]₃Fe₂Br₉ and [4-Br(py)H]₃Fe₂Br₉ (Figure 7) are almost identical over the entire temperature region of the experiment. The difference in the transition temperatures between the two compositions results in

Table I. Transition Temperatures and Magnetic Entropies As Determined by Specific Heat and ac Susceptibility

composition	T_{c1}/K		$S_{\text{mag},m}^-$ (T_{c1})/ R	T_{c2}/K		$S_{\text{mag},m}^-$ (T_{c2})/ R
	χ	C_p		χ	C_p	
[4-Cl(py)H] ₃ Fe ₂ Br ₉		5.50	1.935	7.96	7.92	2.908
[4-Br(py)H] ₃ Fe ₂ Br ₉		5.23	1.764	7.73	7.635	2.846
[4-Cl(py)H] _{1.1} [4-Br- (py)H] _{1.9} Fe ₂ Br ₉	7.73	7.52	2.15	7.78	7.80	2.39

the small difference in the magnetic entropies between T_{c1} and T_{c2} . The remarkable similarity of the magnetic entropies for the two compositions, in spite of the small difference in the transition temperatures, leads to a conclusion that the exchange mechanisms are similar. We note that the lattice specific heat of [4-Cl(py)H]₃Fe₂Br₉, and consequently the lattice entropy, are lower, at all temperatures, than those of [4-Br(py)H]₃Fe₂Br₉.

The behaviors of the magnetic susceptibilities of [4-Br(py)H]₃Fe₂Br₉ (Figure 5) and [4-Cl(py)H]₃Fe₂Br₉² are similar (with the exception of the shift in the transition temperature from 7.96 to 7.73 K upon substituting Br for Cl). A comprehensive discussion on the magnetic susceptibility of [4-Cl(py)H]₃Fe₂Br₉ and its implications is given elsewhere.² That discussion is applicable to the magnetic susceptibility of [4-Br(py)H]₃Fe₂Br₉ as well and shall not be repeated here.

The λ -type transition at 5.23 K is identifiable only in the specific heat data. No indication for a magnetic transition at that temperature is found in the ac susceptibility data, regardless of crystal orientation. No change in the out-of-phase signal is found at that temperature either. This result is similar to that found for [4-Cl(py)H]₃Fe₂Br₉. We note that the absence of an anomaly in the magnetic susceptibility of [4-Cl(py)H]₃Fe₂Br₉ to coincide with the transition at 5.50 K served as one of the more important motivations for studying [4-Br(py)H]₃Fe₂Br₉. From $T_{c1} = 5.23$ K, we calculate $J/k_B = -0.21$ K. The transition temperatures and other data are summarized in Table I.

(d) Exchange Mechanisms. The magnetic ordering phenomena in the three compositions are predominantly long-range in nature, as is evident from the magnetic entropy distributions. Earlier² three possible mechanisms for magnetic exchange interaction were proposed: type I, Fe-X...X'...X-Fe, where X' is the ring halide; type II, Fe-X...X-Fe, with no involvement of the ring halide; and type III, Fe-X...Fe. Both type II and type III exchange pathways should have similar (and minor) dependences on the nature of the ring halide, resulting in a small drop in the transition temperature upon substituting Br for Cl. The halide dependence of the type I pathway is expected to be much stronger. The dependence of the transition temperatures on the ring halide upon substitution from [4-Cl(py)H]₃Fe₂Br₉ to [4-Br(py)H]₃Fe₂Br₉ for both transitions is consistent with both type II and type III interactions. That leads us to conclude that type I exchange through the pyridinium ring halide is not supported by the experimental observations. Type III exchange, which results in a dimer-like exchange mechanism, is likewise not supported by the experimental evidence. Eight possible type II channels were identified in ref 2. These consist of four channels measuring 8.8 Å or more and four channels measuring about 8.6 Å.

The ordering mechanisms in [4-Cl(py)H]₃Fe₂Br₉ and [4-Br(py)H]₃Fe₂Br₉ are similar, as is apparent from the morphology of the transitions and the entropy distributions (Figure 7). The small shift in transition temperatures is attributed solely to the change in the length of the exchange pathways upon chemical substitution. The presence of two ordering temperatures in each of these compounds is surprising, however. More than a single ordering temperature at zero external field is rare among coordination compounds. An example that comes to mind is

$\text{NiCl}_2 \cdot 2\text{H}_2\text{O}$,¹² whose magnetic phase diagram reveals two antiferromagnetic phases belonging to two different space groups.¹³ Several ordering temperatures are also found for several Mn_xO_y minerals,¹⁴ CuO ,^{15,16} $\text{MnAs}_{1-x}\text{P}_x$,¹⁷ and several lanthanide compounds such as PrCo_2Si_2 ,¹⁸ and CeSb .¹⁹ Two ordering temperatures and a first-order transition associated with a structural change at T_{c1} are found for $\text{Mn}_x\text{Cr}_{1-x}\text{As}$.²⁰ It is therefore evident that both $[\text{4-Cl(py)H}]_3\text{Fe}_2\text{Br}_9$ and $[\text{4-Br(py)H}]_3$

Fe_2Br_9 exhibit two canted antiferromagnetic phases belonging to two different space groups where neither the canting angle nor the easy axis changes between these phases.

The mixing of $[\text{4-Cl(py)H}]^+$ and $[\text{4-Br(py)H}]^+$, as in $[\text{4-Cl(py)H}]_{1.1}[\text{4-Br(py)H}]_{1.9}\text{Fe}_2\text{Br}_9$, complicates the exchange pathways and reduces the magnetic symmetry. There are four molecular units in a unit cell and the resulting eight $[\text{FeBr}_4]^-$ ions are arranged in four pairs of tetrahedra. The presence of two types of cations may create two classes of $\text{Fe-Br}\cdots\text{Br-Fe}$ interactions: $[\text{4-Cl(py)H}]_3\text{Fe}_2\text{Br}_9$ -like and $[\text{4-Br(py)H}]_3\text{Fe}_2\text{Br}_9$ -like, which are found to order independently. The two ferromagnetic peaks in the magnetic susceptibility occur in measurements taken with the magnetic field parallel to the b axis, indicating canting toward that axis, with c as the easy axis. It is evident that only a portion of the moments are canted toward the b axis at 7.80 K and that the rest of the moments become canted only at 7.52 K, causing the two ferromagnetic peaks. The lower magnetic symmetry prevents the transition to the lower temperature phase at about 5.5 K.

Acknowledgment. This research was supported by the Solid State Chemistry Program of the Division of Materials Research of the National Science Foundation, under Grant DMR-8815798.

- (12) Polgar, L. G.; Herweijer, A.; de Jonge, W. J. M. *Phys. Rev. B* **1972**, *5*, 1957.
 (13) Swüste, C. H. W.; Botterman, A. C.; Millenaar, J.; de Jonge, W. J. M. *J. Chem. Phys.* **1977**, *66*, 5021.
 (14) Robie, R. A.; Hemingway, B. S. *J. Chem. Thermodyn.* **1985**, *17*, 165.
 (15) Junod, A.; Eckert, D.; Triscone, G.; Müller, J.; Reichardt, W. *J. Phys.: Condens. Matter* **1989**, *1*, 8021. Loran, J. W.; Mirza, K. A.; Joyce, C. P.; Osborne, A. J. *Europhys. Lett.* **1989**, *8*, 263.
 (16) Forsyth, J. B.; Brown, P. J.; Wanklyn, B. M. *J. Phys. C: Solid State Phys.* **1988**, *21*, 2917.
 (17) Laban, A. K.; Westrum, E. F., Jr.; Fjellvåg, H.; Grønvold, F.; Kjekshus, A.; Stølen, S. *J. Solid State Chem.* **1987**, *70*, 185.
 (18) Takeda, K.; Kensuke, K.; Deguchi, H.; Iwata, N.; Shigeoka, T. *J. Phys. Soc. Jpn.* **1991**, *60*, 2538.
 (19) Kasaya, M.; Tani, T.; Iga, F.; Kasuya, T. *J. Magn. Magn. Mater.* **1988**, *76-77*, 278.
 (20) Komada, N.; Westrum, E. F., Jr.; Fjellvåg, H.; Kjekshus, A. *J. Magn. Magn. Mater.* **1987**, *65*, 37.